Marker-controlled picture segmentation applied to electrical logging images

J.F. Rivest*, S. Beucher*, J.P. Delhomme**

* Centre de morphologie mathématique, Ecole des Mines de Paris
35, rue Saint-Honoré 77305 Fontainebleau, France

** Etudes et Productions Schlumberger
26, rue de la Cavée B.P. 202, 92142 Clamart CEDEX, France

ABSTRACT

This paper presents an application of marker-controlled segmentation in petroleum engineering. The images to be segmented originate from high resolution conductivity measurements of borehole walls. These measurements reflect the composition and structure of the rock formation through which the well was drilled. In this application, we detect and measure small cavities in the walls.These cavities are called vugs.

We use the tools provided by mathematical morphology. Our strategy is based on gradient image modification using markers and on the watershed transformation. First, the vugs are automatically marked, as well as the background. These markers together delineate areas of interest in which we know there is one contour per vug. In order to find the vug contour and perform measurements, we modify the gradient image in such a way that only a single edge is kept between the vug and the background markers. We perform the final step of edge detection using the watershed transformation of the modified gradient image. The final result is one closed contour per marked vug.

We present this strategy in detail, show experimental results and discuss artifact elimination.

1 INTRODUCTION

There exist two basic approaches to image segmentation. The first one is boundary-based and finds local changes. The second is region-based and searches for pixel and region similarities[18 10]. They both attempt to degrade image data as gracefully as possible to extract tokens to be passed to higher level analyzers.

The most widely used set of tokens is the edge map: objects in images are represented using their edges, giving a cartoon-like representation of them. There are good reasons to adopt this image representation. From a computational point of view, an edge map neatly represents image data: it is compact and we may devise powerful algorithms to extract and integrate from it higher-level characteristics such as length, curvature and so on. This representation is also consistent with experimental results from physiology, which tend to confirm the existence of such mechanism in vision processes[12].

In this application, the approach proposed by Marr and Hildreth[12 13] to obtain a cartoon-like representation is inoperative as it experiences two implementation problems. The first of these problems originates from the implementation of the edge finder. It is not a trivial task and most of the approaches used to achieve this goal need parameters to be carefully adjusted for a specific application. An example of edge finder is the thresholding of gradient images[1]. It is very sensitive to noise and threshold parameters, and gives thick and incomplete edges.

A more sophisticated algorithm uses heuristic search[11 14]. It gives better results, but we have to define the heuristics, cost functions, start and stop criteria with care. These heuristics vary from an application to another and it may be difficult to find good heuristics to make it work. Edge finding using zero-crossings of the second derivative of images is sensitive to noise and quantification errors. Blurring filters may be used to improve the SNR and regularize the ill-posed problem of derivation[8], but their action is antagonist with edge detection. Moreover, the use of these filters imply an a priori knowledge of object size. In our application, this knowledge is not available.

In order to give an answer to the problem of finding edges in images, Beucher and Lantuéjoul[6] proposed the use of the watershed transformation on gradient images. It is a powerful approach,but it experiences difficulties not much different from the second problem of Marr's cartoon-like representation: there are too many edges and we must find a strategy to eliminate them. Figure 1 shows this over-segmentation problem in a borehole image.

To overcome these problems, a strategy has been recently proposed by Meyer and Beucher [3 15]. This strategy is called marker-controlled segmentation and has been successfully applied on electrophoresis gel characterization[2 3], road detection[5] and cardiology[9]. The main idea underlying this approach is that often machine vision systems "know" roughly from other sources the location of the objects to be segmented.

The way to apply this approach is the following: first, we find properties which will be used to mark the objects. We call these markers *object markers*. We do the same for the background, i.e, for portions of the image where we are sure there is no pixel belonging to any object. These markers constitute the *background markers*. The remaining of the procedure is straightforward and is the same for all applications: we modify the gradient image in order to only keep the most significant contours in the areas of interest between the markers. Then, we perform on the modified gradient image final contour search using the watershed transformation. No supervision, no parameter and no heuristic is needed to perform the final segmentation. The parameters controlling the segmentation are concentrated in the marker construction step where it is easier to control and validate them.

We used this approach on a specific application from the oil industry. Sections 2-4 describe the application, while section 5 presents the results we obtained from our approach. We expose details on the application which may seem superfluous in a vision paper. However, these details illustrate how we approached the problem, and may show how a generalization can be done for other vision tasks.

2 ACQUISITION

The images were obtained from a Formation MicroScanner™, a tool used in the oil industry to scan borehole walls in order to examine the underlying geological structures[7]. It works by injecting high frequency currents into the formation through an array of electrodes scanning the wall. These electrodes are located on pads which are pressed against the borehole walls by hydraulic devices, as shown on figure 2. Current intensities are acquired, measuring geological formation conductivities. Images are generated by the moving array of electrodes. Pixel grey levels are a representation of the rock formation conductivity, and the whole acquisition process has to be modelled in order to make quantitative measurements on the images. It is in this way that it is an unusual vision problem: we had to use knowledge about the tool response instead of the usual assumptions made for scene analysis[12] which are related to the eye/brain response.

The images are an internal unwrapped view of the borehole walls, the image x axis being the angle θ in a cylindrical coordinates system, while the z axis is associated with depth. Due to the limited pad width, we do not have a complete view of the wall. We have instead stripes corresponding to the acquisition pads. Stripe width is 27 pixels, each pixel representing a square of 2.5×2.5 mm. Figure 3 shows a typical image obtained with this tool.

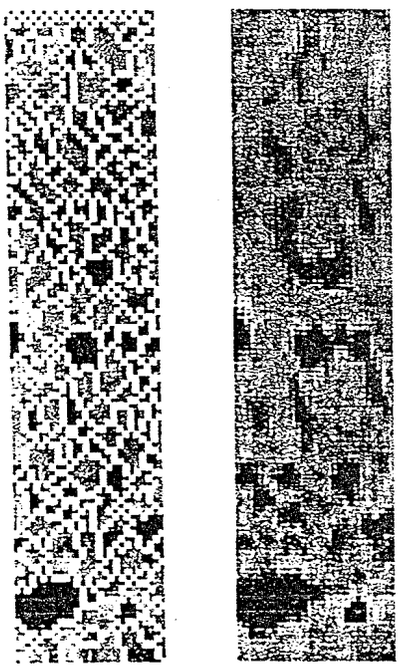

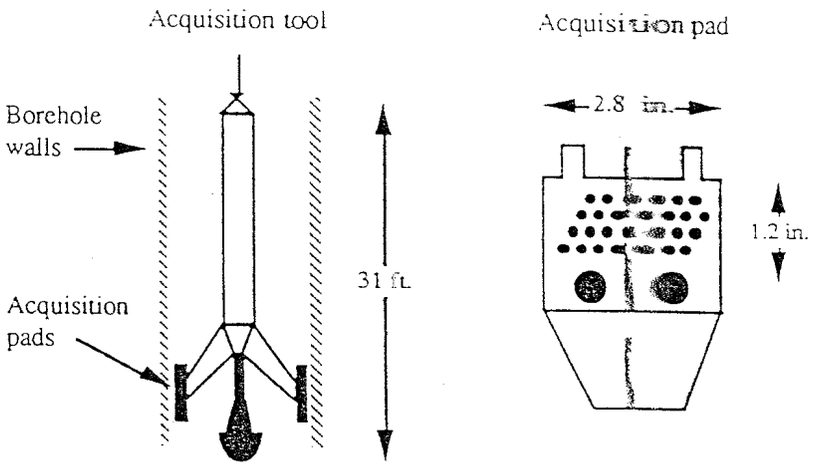

Figure 2: Acquisition tool principle: on the left, the tool scans the walls of a well. On the right, schematic closeup of one pad. Dark circles represent electrodes. (Not to scale.)

Figure 1 (right) and 3 (left): Watershed transformation of gradient images lead to over-segmentation as we see it on this "edge map" put over the typical input image on the left. Height is about 30 cm.

The application is devoted to vug detection in these images. Vugs are small cavities in the rocks and can be compared as pores in a sponge, allowing oil and gas to be stored into the formation. During the drilling process, these vugs are filled with conductive mud giving local conductivity maxima in the images. Numerical modelling of the tool response has shown that a vug boundary corresponds to an inflexion line which may be detected using gradient maxima. It is seen as a crest line in gradient modulus images. Further modelling results show that there is a relationship between conductivity contrast, detected size and vug depth. These result will enable us to qualify in terms of depths the vugs we detect. It is also useful for artefact elimination, as we will show in section 4. Figure 4 shows a typical image profile.

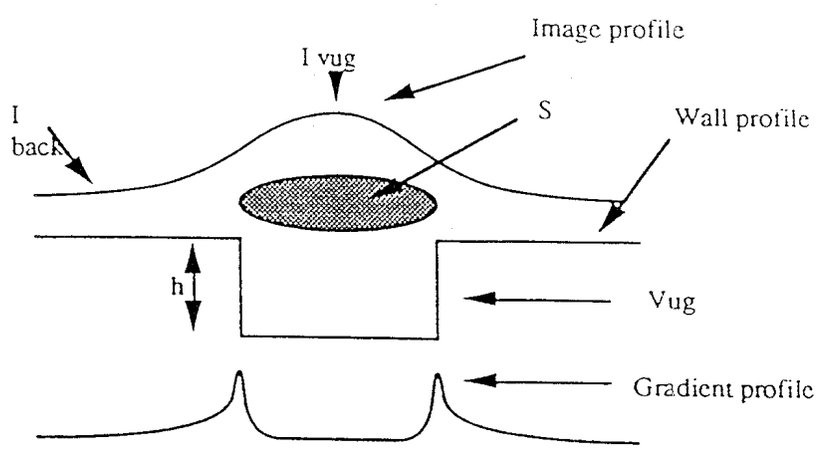

Figure 4: Typical image profile caused by a vug. Top: image profile, middle: underlying vug, bottom, gradient profile.

1451 29

3 PROCESSING

From these criteria, we have to find robust detectors. We describe in this section how we found them. We then detail the algorithms.

3.1 Preprocessing

We resort to filtering in order to generate reliable vug markers. In this application, we use morphological closing $\phi(f)$ with a diamond-shaped structuring element, f being the input image.

The preprocessing steps may vary. For example, we could have used linear filters instead of the closing filter. This is not critical to our application, although morphological closing performed better in our case. There are no straightforward procedures to find good filters yet.

3.2 Marker images generation

Markers play a central role in the approach we present here. This section describes the algorithms we used to get them. In our approach, the markers determine the final segmentation.

Object markers

As we saw in section 2, a vug is seen as a local maximum in conductivity images. The choice among maxima detection algorithms is not critical, if they fulfil the following requirements:

- There must be a unique marker per object: more than one marker will lead to over-segmentation.
- The marker must be located inside the object.

Mathematical Morphology provides an excellent maxima detector[3]. A maximum is a region or a connected component of pixels on an image there is no descending path going to. The detector is implemented as follows:

$$Om = a - recons(a, a\text{-}1), \tag{1}$$

where a is the preprocessed image $\phi(f)$, Om the object marker function and $recons(a,g)$ is the morphological function reconstruction operator. This operator is implemented this way in the digital case:

$$recons(m,a) = min((m \oplus B),a), \textit{ until stability}. \tag{2}$$

$(m \oplus B)$ is the dilation of the marker function m by the planar structuring element B which is the digital disk of diameter 1. The result of each iteration is put back into m. Figure 5 illustrates how the maxima detector works.

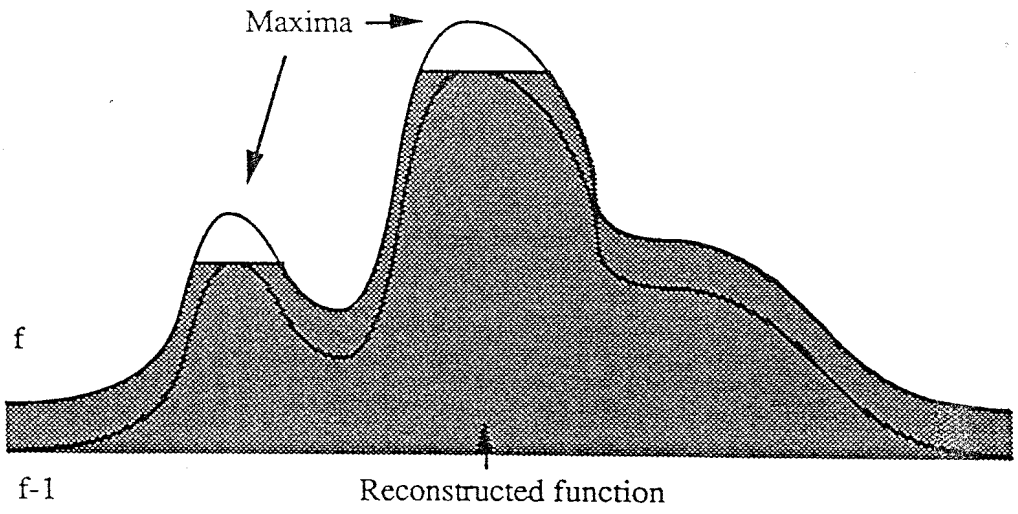

Figure 5: Morphological maxima detector.

Background markers

Between vugs, there are valleys in the conductivity images where pixel intensity is lower. These valleys are not part of the vugs. They form contours of the areas of interest isolating each vug. Again, the choice among many detectors is not critical, provided the following requirements:

- There must not be any object and background marker contact nor overlap.
- The background marker must not lie over the object. It delimits an area of interest in which the object is.

As background marker *Bm*, we used the watershed of the inverse of the filtered image *a*:

$$Bm = watershed(-a) \quad (3)$$

The watershed transformation comes from an analogy of image data with the surface of a landscape, as shown in [3] and [16]. This landscape has peaks, valleys, crestlines and catchment basins. If we let fall water on this surface, it will concentrate over the minima of the surface. The surface drained by a minimum is called a *catchment basin*, and the common points between catchment basins are part of a network called the *watershed* [6].

In practice the algorithms do not work using this definition. They use instead the notion of surface immersion. We can imagine the surface progressively immersed into water, in the same way as we threshold an image. Water will go up through the minima of the image, making ever-increasing lakes which are labelled from the start. At a certain time depending on the altitude of the points, lakes can merge. If we build dams in order to keep the lakes separated, and if we continue flooding the surface, we will end up with lakes separated with dams covering the surface. These dams are the watershed lines. Soille and Vincent[17] recently made a very efficient implementation of the algorithm outlined here. The final segmentation using this algorithm results in compact regions separated by connected lines one pixel wide.

In our case, as we calculate the watershed on the complementary of the filtered image, we find the valleys surrounding maxima, or summits, of the image.

Both markers are united to form the complete marker image *Mf*:

$$Mf = Bm \cup Om. \quad (4)$$

We show on figure 9 the shape and background markers superimposed on the original image.

3.3 Gradient modification

Using the markers, we now eliminate the spurious edges in the gradient image. This is achieved again by morphological function reconstruction. This operation directly manipulates the gradient in such a way that only the strongest edge between the markers will generate a detectable contour for the final search algorithm. This time, instead of reconstructing the function using a marker under the function to be reconstructed, we use a marker which is over it, and work on the complementary of the reconstructed function. By duality, instead of using dilation of the markers followed by intersection with the function to be reconstructed, as in equation (2), we use erosion of the marker function, followed by union of the result with the function to be reconstructed. This dual image reconstruction is implemented as:

$$drecons(m,g) = max((m \ominus B), g), \textit{ until stability.} \quad (5)$$

$(m \ominus B)$ being the erosion of the marker function m by the planar structuring element B which is the digital disk of diameter 1.

Let A be the grey-level function originating from Mf:

$$A = - k_{Mf} + g_{max} (1 - k_{Mf}), \quad (6)$$

g is the gradient image, g_{max} being the maximum value of the image g. k_{Mf} is the indicator function of Mf.

The filtered gradient image is then:

$$G_{final} = drecons(A,g). \quad (7)$$

Figure 6 illustrates how it works.

In the case of the maxima detector, the reconstruction had the effect of clipping peaks. In this case, it fills spurious minima and keeps only pertinent maxima of the function.

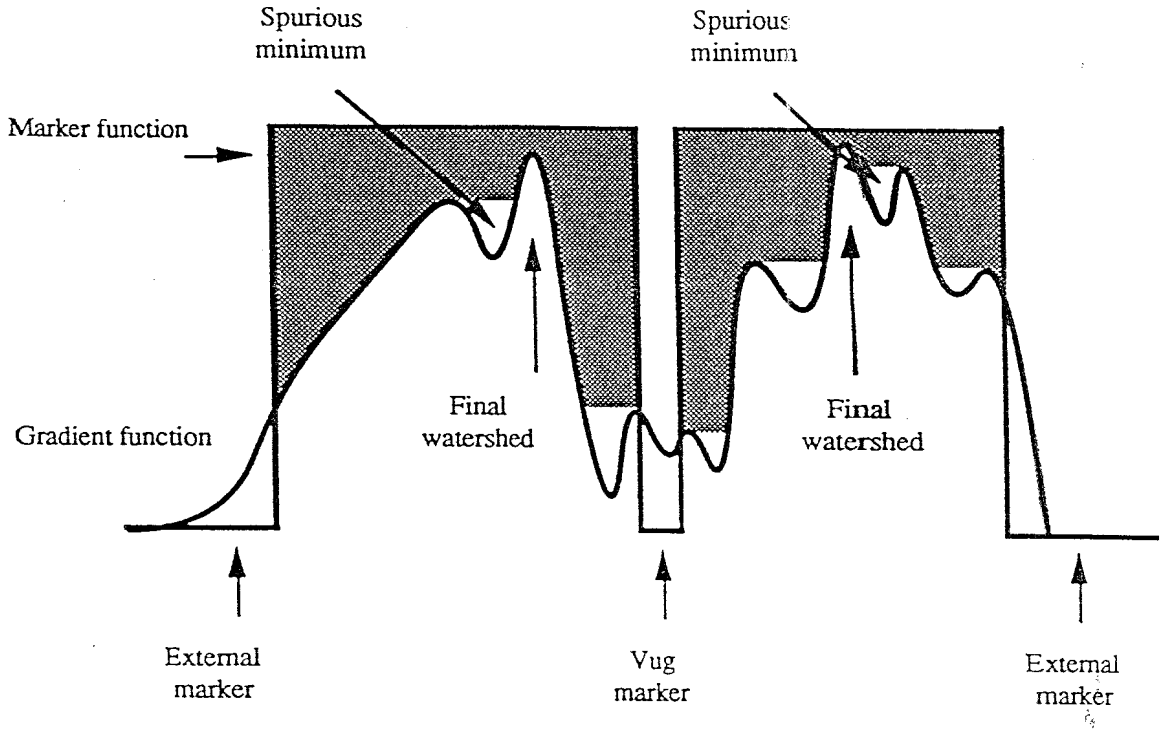

Figure 6: The gradient modification is controlled by the marker function in order to suppress spurious minima leading to over-segmentation.

3.4 Contour extraction

The gradient function being morphologically reconstructed, it is now possible to perform the final contour extraction. The watershed transformation has been proposed by Beucher and Lantuéjoul [6 4] to perform the task. The most similar approach to track contours on gradient images is from Martelli[14] who used heuristic graph search on the image. The watershed transform has the advantage over the former to be non-parametric: there is no threshold or parameter to set and no heuristic to implement. Moreover, it is a global algorithm intrinsically giving closed and thin contours.

$$\text{vug-contours} = \text{watershed}(G_{\text{final}}) \tag{8}$$

4 ARTEFACT ELIMINATION

We experienced a problem while using the maxima detector to mark vugs: homogeneous regions exhibit smooth bumps which are not vugs. As these bumps do not have as much contrast as real vugs, it is possible to threshold markers against image background.

The problem is how to evaluate this background. Interpretation geologists have isolated a few criteria defining the background of conductivity images. The background is associated with large plateaus which are neither maxima nor minima. These plateaus vary smoothly. Generally, background has a relatively low intensity.

From these criteria, we constructed a detection algorithm based on morphological filtering. First, we eliminate image minima smaller than a given size using an closing ϕ: we perform a dilation on the image followed by morphological dual reconstruction. Then, we eliminate maxima on the resulting image using an open-

ing γ: we erode the image and then perform dual morphological reconstruction. The pixels of the image which have not changed are then considered as belonging to the background. The structuring elements used are rectangles spanning the entire width of the image and 40 pixels deep. Figure 7 shows an example of background profile and how the detection algorithm works. This gives us an adaptive threshold. This will not have any influence on the detection in the other zones delimited by the background marker. The filter equations are as follows:

$$\Psi(a) = \gamma(\phi(a)) \tag{9}$$

$$\gamma(a) = recons((a \ominus R), a)) \tag{10}$$

$$\phi(a) = drecons((a \oplus R), a) \tag{11}$$

where Ψ is the morphological filter, a the input image, *recons* and *drecons* the morphological reconstruction operators and R is the rectangular structuring element we used. Figure 8 shows the different steps of the filter.

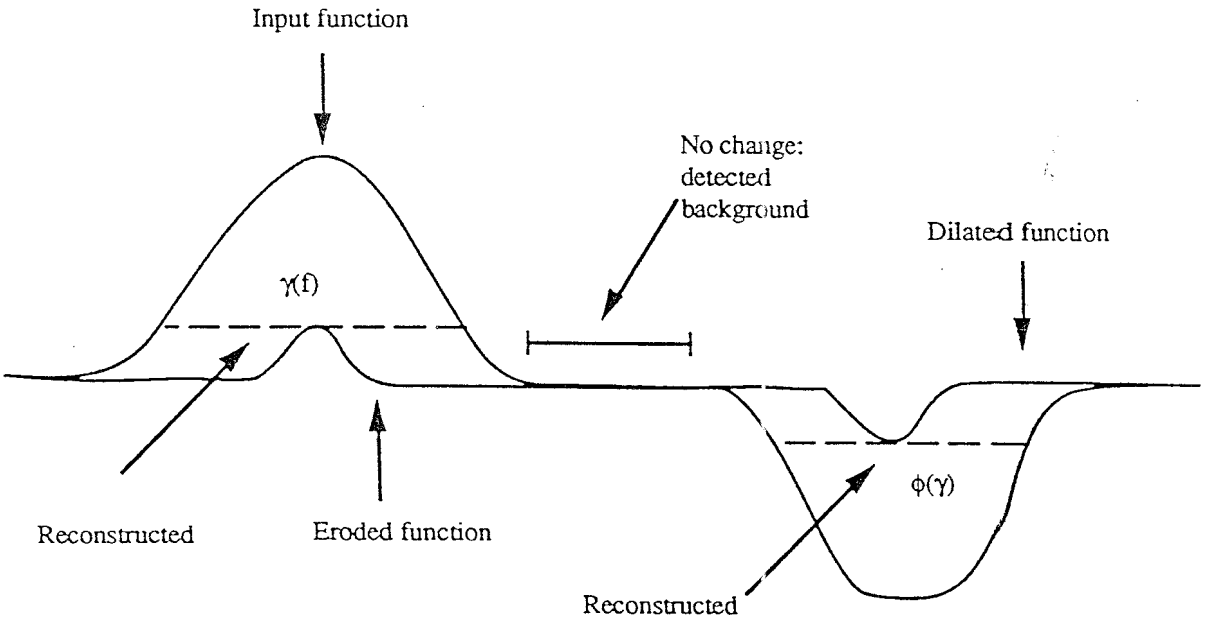

Figure 7: Background detection by filtering. Plateaus larger than structuring element size are unchanged and considered as background.

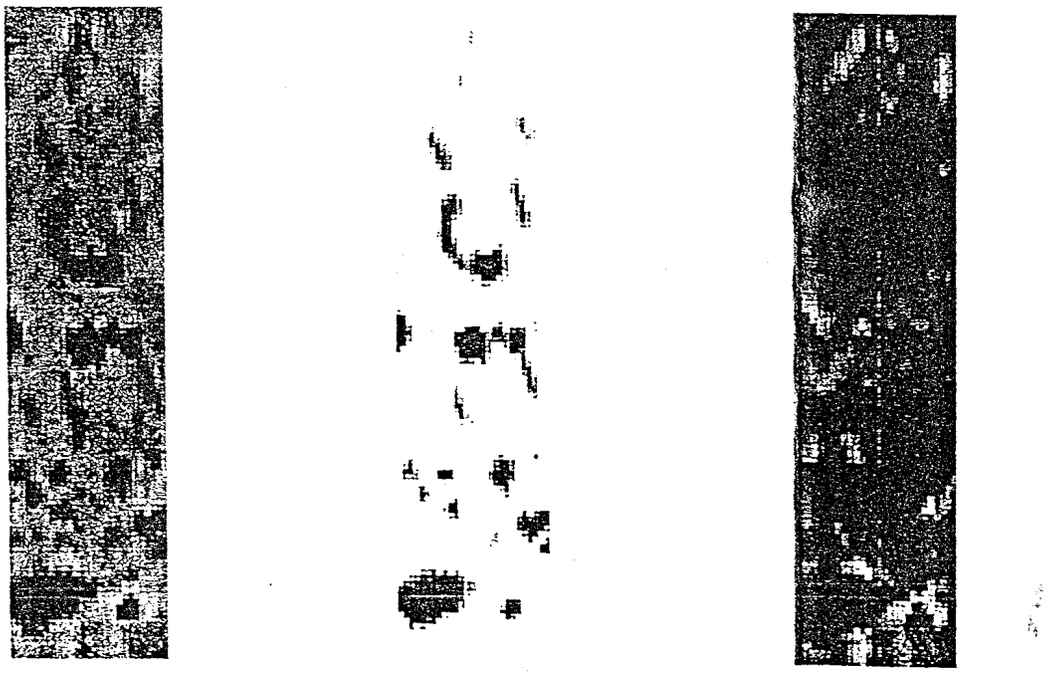

Figure 8: Left: original image, middle: closing with reconstruction, right: opening with reconstruction. The closing eliminate minima smaller than the structuring element used while the opening eliminate maxima.

5 EXPERIMENTAL RESULTS

We first tested the system on lab data obtained from a rock block into which holes of various diameters and depths have been drilled. Results were excellent. In this paper, we present results obtained from real well data originating from a carbonate reservoir. Results correlate well with visual detection. Some differences observed were caused by incorrect artefact elimination. Some contours were slightly shifted compared to the contours found visually, but there were also differences when different geologists contour the vugs by hand. There are two causes to these inconsistencies: the first one is a blurring effect caused by the point-spread function of the acquisition system, which makes a visual ambiguity The second cause is a visualisation artefact: the dynamic range of the images is too wide for a CRT screen and this generates clipping effects which may shift visual boundaries.

Figure 9 shows segmentation results. Validation is still under way in order to compare the results obtained with information gathered from other sensors.

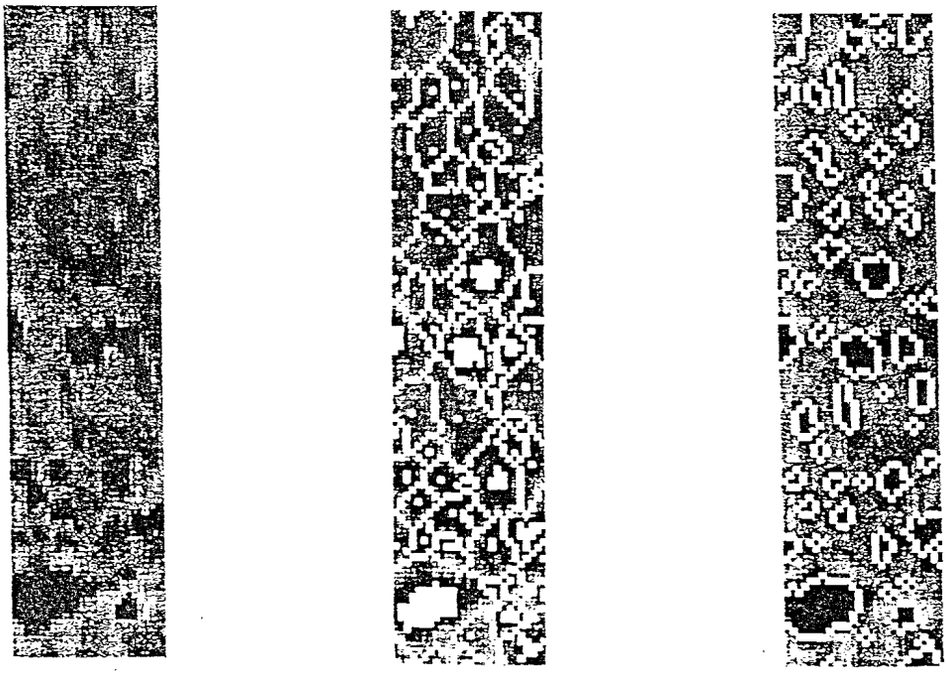

Figure 9:Left: original image, center: vug and background markers over input image, right: contours found by the system.

6 DISCUSSION

The segmentation results are strongly dependent upon the reliability of the markers.

This segmentation strategy has the following advantages:

- Fewer rules and parameters are needed as compared to other techniques.
- A marker is a binary set. It is less complex to process and manipulate than a full grey-level image or a set of filter parameters.
- The approach is more related to the physical world: marker parameters are usually more goal-oriented and physically justifiable than parameters such as thresholds or region growing criteria [10 18].
- The marker generation modules, gradient operators and edge detectors are all independent. The well-admitted principle of modularity mentioned by Marr[12] is respected here. This gives to our strategy the flexibility segmentation systems badly need.
- The user may even put himself the markers on the image. Often, the tedious task for human operators is to measure objects. Recognition is generally not very difficult. Image processing algorithms have usually more problems recognizing objects than measuring them once they are recognized. We can use the strengths of both the operator and the system, letting the operator perform recognition and the algorithm measurements and fine segmentation.

This strategy is rather different from those who were generally proposed in the literature, such as the primal sketch[13]. Image understanding is done at the first place using simple detectors. It is during this marker generation step that most of the "graceful degradation"[12] is done. Contour extraction only aims at measuring objects.

7 CONCLUSION

We have presented an alternative approach to edge detection and region growing segmentation. With the use of objects and background markers, it is possible to suppress spurious edges by directly modifying gradient images before searching for the edges. The boundary is known to be located between the object and background marker surrounding it. The morphological function reconstruction acts as a spurious edge removal transformation. It leaves only the strongest gradient crest between edge and background markers. Afterwards, any straightforward edge follower can be used in order to track the edge left by the reconstruction step. The watershed transformation by construction gives thin and closed contours.

This segmentation strategy has the advantage of restricting the parameter setting process to the marker generation step. This makes the overall algorithm more robust and modular. It is then easier to validate, develop and maintain.

8 REFERENCES

[1] I.E. Abdou, W.K. Pratt, "Quantitative Design and Evaluation of Enhancement / Thresholding Edge Detectors", *Proceedings of the IEEE*, Vol. 67, No. 5, pp. 753-763, 1979.

[2] S. Beucher, "Lecture automatique des gels d'électrophorèse", *Technical Report. Centre de Géostatistique et Morphologie Mathématique, Ecole des Mines de Paris, No.* N-746, 1982.

[3] S. Beucher, "Segmentation d'images et morphologie mathématique", *Ph. D. Thesis, Ecole des Mines de Paris, 1990.*

[4] S. Beucher, "Watersheds of Functions and Picture Segmentation", *ICASSP 82, Proceedings IEEE International Conference on Acoustics, Speech and Signal Processing*, pp. 1928-1931, 1982.

[5] S. Beucher, M. Bilodeau, X. Yu, "Road Segmentation by Watershed Algorithms", *PROMETHEUS Workshop, 1990.*

[6] S. Beucher, C. Lantuéjoul, "Use of Watersheds in Contour Detection", *International Workshop on Image Processing: Real-Time Edge and Motion detection/estimation*, 1979.

[7] M.P. Ekstrom, C. Dahan, M.-Y. Chen, P. Loyd, D. Rossi, "Formation Imaging with MicroElectrical Scanning Arrays",*The Log Analyst*, Vol. 28, No. 3, pp. 294-306, 1987.

[8] E. De Micheli, B. Caprile, P. Ottonello, V. Torre, "Localization and Noise in Edge Detection", *IEEE Transactions on Pattern Analysis and Machine Intelligence*, Vol. 11, No. 10, pp. 1106-1116, 1989.

[9] F. Friedlander, "Le traitement morphologique d'images de cardiologie nucléaire", *Ph. D. Thesis, Centre de Morphologie Mathématique, Ecole des Mines de Paris*,1989.

[10] A. Gagalowicz, O. Monga, "A new approach for image segmentation", *Proceedings, 8th Int. Conf. Pattern Recognition, Paris, pp. 265-267, (1986).*

[11] J. Lester, H. Williams, B. Weintraub, J. Brenner, "Two graph searching techniques for boundary finding in white blood cell images", *Comput. Bio. Med.* Vol. 8, pp. 293-308, 1978.

[12] D. Marr, "Early Processing of Visual Information", *Proc. R. Soc. Lond.* Vol 275 B. 942 pp. 483-520, 1976.

[13] D. Marr, E. Hildreth, "Theory of Edge Detection", *Proc. R. Soc. Lond.* B 207, pp. 187-217 1980 .

[14] A. Martelli, "Edge detection using heuristic search methods", *Computer vision, Graphics, and Image Processing*, Vol. 1, pp. 335-345, 1971.

[15] F. Meyer, S. Beucher, "Morphological Segmentation", *Journal of Visual Communication and Image Representation*, Vol. 1, No. 1, pp. 21-46, September 1990.

[16] P. Soille, M.M. Ansoult, "Automated Basin Delineation From Digital Elevation Models Using Mathematical Morphology", *Signal Processing*, Vol. 20 pp. 171-182, 1990.

[17] P. Soille, L. Vincent, "Determining watersheds in digital pictures via flooding simulations", *Proceeding SPIE Vol. 1360 Visual Communications and Image Processing '90 October 1990.*

[18] S. W. Zucker, "Region Growing: Childhood and Adolescence", *Computer Graphics and Image Processing* 5, pp. 382-399, 1976.